Clays and Clay Minerals, Vol. 46, No. 5, 567–573, 1998.

$^{131}I^-$ SORPTION BY THERMALLY TREATED HYDROTALCITES

MARÍA TERESA OLGUÍN,[1] PEDRO BOSCH,[2] DWIGHT ACOSTA[3] AND SILVIA BULBULIAN[1]

[1] Instituto Nacional de Investigaciones Nucleares, A.P. 18-1027, Col. Escandón, Delegación Miguel Hidalgo, C.P. 11801, México, D.F.

[2] Universidad Autónoma Metropolitana, Iztapalapa, Michoacán y Purísima, A.P. 55-532, Iztapalapa, C.P. 09340, México, D.F.

[3] Universidad Nacional Autónoma de México, Instituto de Física de la UNAM, Ciudad Universitaria A.P. 70-360, C.P. 04510, México, D.F.

Abstract—The sorption capacity of hydrotalcite (HT) and its calcined product (CHT) was evaluated for $^{131}I^-$ sorption from water solution and it was determined as a function of the calcining temperature. The radionuclide content was determined by γ-spectrometry. Solids were characterized by thermal analysis, X-ray diffraction (XRD), electron microscopy and Brunauer-Emmett-Teller (BET) analysis. For 0.1 *M* Na I solution, labeled with $^{131}I^-$, sorption capacity was found to be 0.24 meq g^{-1} (7.2% of the anion exchange capacity, AEC). But, if the sample was previously calcined at 773 K and the HT structure destroyed, the sorption of I^- increased considerably, up to 2.08 meq g^{-1} (63% of the AEC) and the HT structure was reconstructed. The $^{131}I^-$ sorption at very low concentrations (10^{-14} *M*) was 0.04×10^{-14} meq of $^{131}I^-$ g^{-1} in the noncalcined HT, but for calcined samples at 773 K, the sorption increased to circa 0.97×10^{-14} meq g^{-1}. Calcination temperature determines the surface area of the resulting mixed oxides, and that property seems to be the most important factor controlling the I^- sorption. If the calcination temperature was increased to 873 K, the specific surface area of the oxide mixture increased and I^- sorption increased as well, whereas calcination of HT at 973–1073 K resulted in a low surface area and a low I^- retention.

Key Words—Hydrotalcites, $^{131}I^-$, $^{131}I^-$ Sorption, Anion Exchange, Magnesium Aluminum Oxide, Radioactive Waste, Radioactive Decontamination, Thermal Treatment.

INTRODUCTION

A topic of particular interest in the sorption of anions is the decontamination of wastewater (Olguín 1994; Olguín et al. 1996). Atkins and Glasser (1990) studied the encapsulation of radioiodine in cementitious waste forms. They presented data on the uptake of the I^- on specific phases: $Ca(OH)_2$, aluminate sulfate hydrates, HT and Ca silicate hydrogel. The HT compounds consist of positively charged brucite-like octahedral hydroxide layers, which are neutralized by anions and water molecules occupying the interlayer space. Magnesium atoms (Mg^{2+}) in HTs are octahedrally coordinated to the surrounding hydroxide ions and share adjacent edges to form sheets of layers. Some of the magnesium is isomorphously replaced by aluminum (Al^{3+}), which produces net positive charges on the metal hydroxide layers as Al^{3+} remains octahedrally coordinated to the hydroxyl groups. This layer charge, in naturally occurring HT, is balanced by interlayered carbonate. As HTs are laminar and capable of anion-exchange reactions, they can be conceptualized as being the anionic equivalent of cationic clays (Miyata 1973, 1975, 1980, 1983; Kopka et al. 1988; Cavani et al. 1991; Mckenzie et al. 1992).

Sato et al. (1986) have prepared magnesium aluminum oxide solid solutions by thermal decomposition of an HT-like compound. They found that magnesium aluminum oxide hydrated and took up carbonate ions from the aqueous solution to reconstruct the HT-type structure. Sato et al. (1986) also found that the solid solution decomposes above 1273 K to MgO and $MgAl_2O_4$, which showed no capacity to take up anions. The changes that occur during thermal decomposition of HTs were described previously by Miyata 1980; Reichle 1985, 1986; Reichle et al. 1986; and Mckenzie et al. 1992. With increasing temperature, interlayer water is first lost, followed by the dehydroxylation and the decomposition of the interlayer carbonate to CO_2. In addition, the XRD pattern of the resulting oxide indicates an undefined MgO structure with no clear crystalline phases. According to the same authors, removal of CO_2 and structural water from calcined HT is accompanied only by a modest increase in specific surface area.

However, Choudhary and Pandit (1991) found that the surface properties of magnesium HT are strongly influenced by its calcination temperature. Competition between monovalent and divalent anions for calcined and uncalcined HT has also been studied (Chatelet et al. 1996). Hermosin et al. (1996) evaluated the sorption capacity of HT-like compounds and their calcined products and they studied their role as potential filters of various organic compounds present in water, especially those that may exist as anions. Misra and Perrotta (1992) studied the composition and properties of synthetic HTs. They also prepared pillared HTs by molybdate, chromate and silica anion replacement.

The aim of the present paper is to discuss the sorption of radioactive $^{131}I^-$ from aqueous solutions by HTs, either dried or calcined. Thermal decomposition

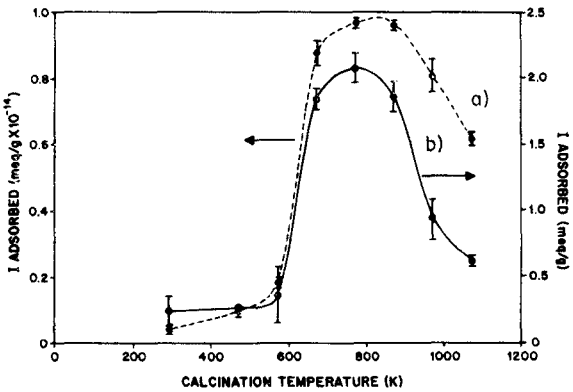

Figure 1. Sorption of I^- from a) 10^{-14} *M* NaI and b) 0.1 *M* NaI- ^{131}I solutions.

of the synthetic HT compounds and their structure before and after being in contact with NaI solutions were investigated by XRD, thermal analysis, N_2 adsorption (BET) and electron microscopy.

MATERIALS AND METHODS

Preparation of HT Samples

Hydrotalcite, $Mg_{3/4}Al_{1/4}(OH)_2)(CO_3)_{1/8}\cdot 0.5H_2O$, whose AEC was 3.3 meq g^{-1}, was prepared as described previously by Sato et al. (1988): 1 L of a mixed aqueous solution of $MgCl_2$ and $AlCl_3$ was added continuously to 1 L of a mixed aqueous solution of NaOH and Na_2CO_3 ($Na^+/(2Mg^{2+} + 3Al^{3+}) = 1.1$; $(CO_3^{2-}/Al^{3+}) = 2$ at 333 K). The mixtures were stirred during reaction. The precipitate was washed at 291 K until Cl^--free and dried at 353 K for 48 h. The HT samples prepared and dried as previously described were calcined in air at temperatures from 473 to 1073 K for 5 h (samples 473CHT to 1073CHT).

HT Characterization

Hydrotalcites were characterized by thermal analyses, XRD, electron microscopy and BET analyses.

THERMAL ANALYSES. Thermogravimetric analysis (TGA) was carried out with a TGA 51 TA Instruments thermogravimetric analyzer, which was operated in a N_2 atmosphere and at a heating rate of 10 K min^{-1} from 298 to 1073 K.

XRD. The powder diffractograms were obtained with a Siemens D500 diffractometer coupled to a copper anode X-ray tube. The $K\alpha$ radiation was selected with a diffracted beam monochromator. Compounds were identified comparing with the Joint Committee on Powder Diffraction Standards (JCPDS) cards in the conventional way. The (006) hydrotalcite peak was chosen as it is the closest peak to the corundum (α-Al_2O_3) peaks used as an internal standard.

ELECTRON MICROSCOPY. Conventional transmission electron microscopy (CTEM) techniques were used to study the morphology and structural details of HTs before and after exchange with I^- ions. Before mounting in the microscope specimen camera, the samples were ground in an agate mortar. Then they were dispersed in isopropyl alcohol using an ultrasonic bath and deposited over 200-mesh copper grids covered with a holey carbon film. Observations were carried out in a side entry JEOL 100 CX microscope.

Scanning electron microscopy (SEM) was used to determine topological and surface configurations of HT before and after the I^- exchange process; the samples were dispersed by ultrasound, deposited in SEM holders and covered with sputtered gold to avoid charging effects during observation. SEM micrographs were obtained in a JEOL 5200 scanning microscope. Mean particle size was estimated from the obtained SEM micrographs.

BET ANALYSIS, SURFACE AREAS. The BET surface areas were determined by standard multipoint techniques, Micromeritics Gemini 2360 instrument. The samples were dehydrated at 473 K.

$^{131}I^-$ Sorption

A carrier-free Na ^{131}I solution (10^{-14} *M* I^- solution) and a 0.1 *M* NaI labeled with ^{131}I (NaI-^{131}I) solution were used in the experiments. These conditions were found to be appropriate for our experiments, as they covered the very low and high I^- concentration ranges, respectively.

In the test for I^- uptake from aqueous solution, HT or CHT samples were left in contact with either the carrier-free (NaI-1) or the 0.1 *M* NaI-^{131}I (NaI-2) solutions. The pH value of the NaI-1 solution was 6.1 and the NaI-2 solution, 7.4.

To start I^- uptake, 150 mg of HT or CHT samples were placed in stoppered glass tubes. The samples were left in contact for 24 h with 15 mL of NaI-1 or NaI-2 solution then stirred for 10 s. The samples left in contact with NaI solutions are referred to in this paper as "HT-I" and "CHT-I", respectively. Finally, each solution was separated from the solid by centrifugation and an aliquot was analyzed by γ-spectrometry, using the characteristic ^{131}I photopeak, 0.364 MeV and half life, 8 d. The amount of $^{131}I^-$ sorbed was estimated by determining the difference in activity between the blank of the initial $^{131}I^-$ solution and the corresponding aliquot.

The pH evolution value of NaI solutions before and after the sorption process was measured in an Orion Research Microprocessor Ionaly Zer /901 potentiometer with a combined glass electrode.

RESULTS

$^{131}I^-$ Sorption

In Figure 1, the $^{131}I^-$ uptake on HT samples dried and heated in air from 473 to 1073 K (473CHT to

https://doi.org/10.1346/CCMN.1998.0460510 Published online by Cambridge University Press

Table 1. The pH values of NaI-1 (carrier-free Na ^{131}I) and NaI-2 0.1 *M* NaI labeled with ^{131}I solutions.

Sample	Calcination temperature	pH of NaI-1 solution	pH of NaI-2 solution
HT	—	9.05	9.14
CHT	473	9.35	9.52
CHT	573	9.35	9.58
CHT	673	10.14	11.66
CHT	773	10.54	11.98
CHT	873	10.52	11.99
CHT	973	10.21	11.80
CHT	1073	10.37	11.64

1073CHT) is presented. Curve a) corresponds to the I^- uptake from a carrier-free Na ^{131}I solution (NaI-1) and curve b) from 0.1 *M* NaI-^{131}I solution (NaI-2). In a first step, a very weak $^{131}I^-$ uptake was observed in both cases. From low temperatures up to 573 K, the uptake was almost constant; at 291 K, the I^- uptake was of 0.04×10^{-14} meq g^{-1} (1.2×10^{-14}% of the AEC) for curve a) and of 0.24 meq g^{-1} (7.2%) for curve b). Then it increased rapidly from 673 to 874 K. The maximum uptake circa 0.97×10^{-14} meq g^{-1} (30×10^{-14}%) for curve a) and 2.08 meq g^{-1} (63%) for curve b) was at 773 K. Then a third step was observed where the uptake decreased with increasing calcination temperature down to ca. 0.60×10^{-14} meq g^{-1} (18×10^{-14}%) for curve a) and 0.6 meq g^{-1} (18%) for curve b). The amount of $^{131}I^-$ sorbed by the solid samples was very much dependent on the NaI concentration; however, the shape of the sorption curves was similar for NaI-1 and NaI-2 solutions.

The pH values of the NaI-1 and NaI-2 in contact with HT or CHT samples are reported in Table 1. The final pH value of the solutions depended on the thermal treatment of the HT and, in all cases, it was higher than the initial pH. The pH increase of the NaI-1 and NaI-2 solutions in contact with samples 473CHT and 573CHT was similar to that of sample HT. However, for samples 673CHT, the increase of pH was considerable: 10.54 for NaI-1 solution and 11.66 for NaI-2 solutions. For higher calcination temperatures, the increase in pH of the solutions remained almost constant.

Thermal Analyses

Figure 2 compares a) the original HT weight loss curve and b) the corresponding 773CHT sample and solution left in contact with NaI-^{131}I (sample 773CHT-I). Both curves present 2 clear weight losses. The first one at 473 K was due mainly to loss of interlamellar water, and the second one at 673 K to dehydroxylation with decarbonation (Miyata 1975, 1980; Reichle et al. 1986; Sato et al. 1986; Rey et al. 1992).

XRD

The XRD patterns of the synthetic HT and the corresponding 473CHT to 1073CHT samples for 5 h are

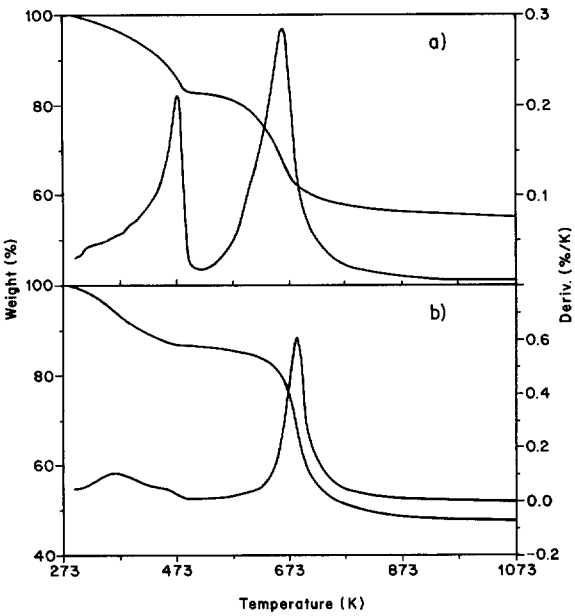

Figure 2. TGA of a) the original HT sample and b) the CHT sample calcined at 773 K and left in contact with 0.1 *M* NaI-^{131}I solution (773CHT-I).

compared in Figure 3. The HT sample showed an HT-type pattern. The same diffraction peaks were observed in 473CHT and 573CHT samples. If the sample was calcined between 673 and 1073 K, the diffractogram corresponded to periclase (MgO) and γ-alumina (Al_2O_3), as observed by Chatelet et al. (1996 and references therein). The HT network was destroyed already at 673 K and, as calcination temperature was increased, the resolution of the MgO (JCPDS card-4-829) peaks improved, showing that crystallite size increased.

These CHT samples, in contact with I^- solution, reproduced the lamellar hydrotalcite structure as shown by the XRD patterns (Figure 3b). The *d*(006) interplanar distances are compared in Table 2. The *d*(006) value is constant and equal to 3.90 Å, as in the original HT sample, even for the 573 K treated sample. The *d*(006) distance increases up to about 4.08 Å if the reconstructed hydrotalcite comes from the 673CHT and 873CHT samples. The (006) interplanar distance decreases to 3.90 Å as the corresponding calcination temperature was 1073 K.

Electron Microscopy

Figure 4 is a CTEM micrograph showing typical details found in an HT sample and CHT sample after I^- exchange. Small grains (marked with arrows), with different thicknesses, supported a second phase. No significant variations in configuration were observed between both samples. Figure 5 is a typical selected area electron diffraction (SAED) pattern. Monocrys-

https://doi.org/10.1346/CCMN.1998.0460510 Published online by Cambridge University Press

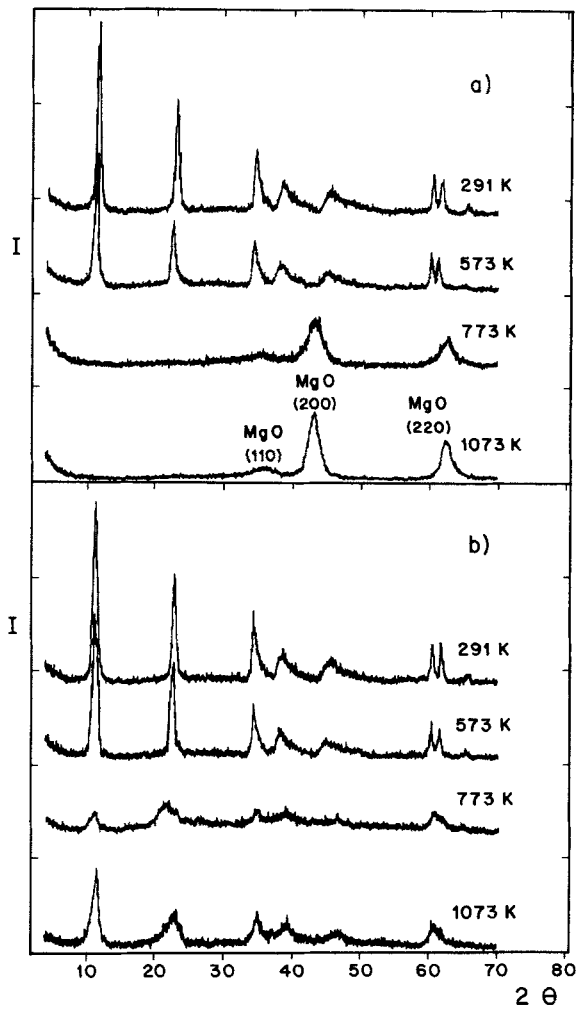

Figure 3. XRD patterns of a) HTs dried or calcined at different temperatures (from 291 to 1073 K) (HT and CHT samples) and b) dried or calcined (from 291 to 1073 K) HTs left in contact with NaI solutions (HT-I and CHT-I samples).

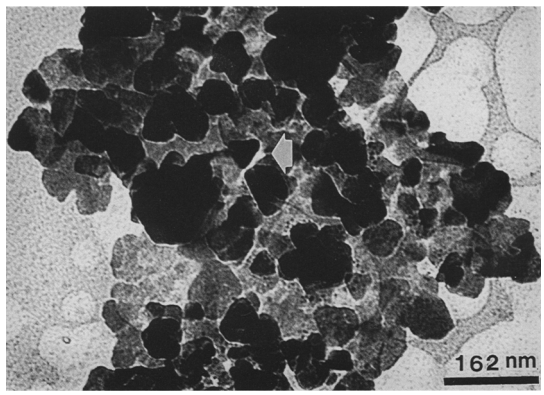

Figure 4. CTEM micrograph of HT sample.

talline and polycrystalline details can be observed in this micrograph, and the interplanar distances derived from this pattern corresponded to those reported for HTs (ICDD 22-700). Figures 6a, 6b and 6c are SEM images from the HT sample and those calcined, 773CHT and 1073CHT samples; no significant variation of the surface of big grains is observed, but an increase in the number and in the size of supported small particles can be appreciated in the mentioned sequence. This behavior is presented graphically in Figure 7.

BET Analysis, Surface Area

HT and CHT surface area was almost constant from room temperature up to 573 K: ca. 100 $m^2\ g^{-1}$. However, as new phases appeared, the surface area increased rapidly up to 220 $m^2\ g^{-1}$ (samples 673CHT and 773CHT). For higher temperatures (873CHT–1073HT samples), the surface area decreased to 150–160 $m^2\ g^{-1}$, as shown in Figure 8.

Table 2. Interplanar distances d(006) for untreated hydrotalcite and for the calcined samples left in contact with 0.1 M NaI-^{131}I solution.

Sample	Calcination temperature of HT	$d \pm 0.01$ Å
HT	—	3.90
CHT	473	3.91
CHT	573	3.91
CHT	673	3.98
CHT	773	4.08
CHT	873	4.07
CHT	973	3.91
CHT	1073	3.91

Figure 5. SAED pattern of CHT sample calcined at 773 K and left in contact with 0.1 M NaI- ^{131}I, 733CHT-I solution.

https://doi.org/10.1346/CCMN.1998.0460510 Published online by Cambridge University Press

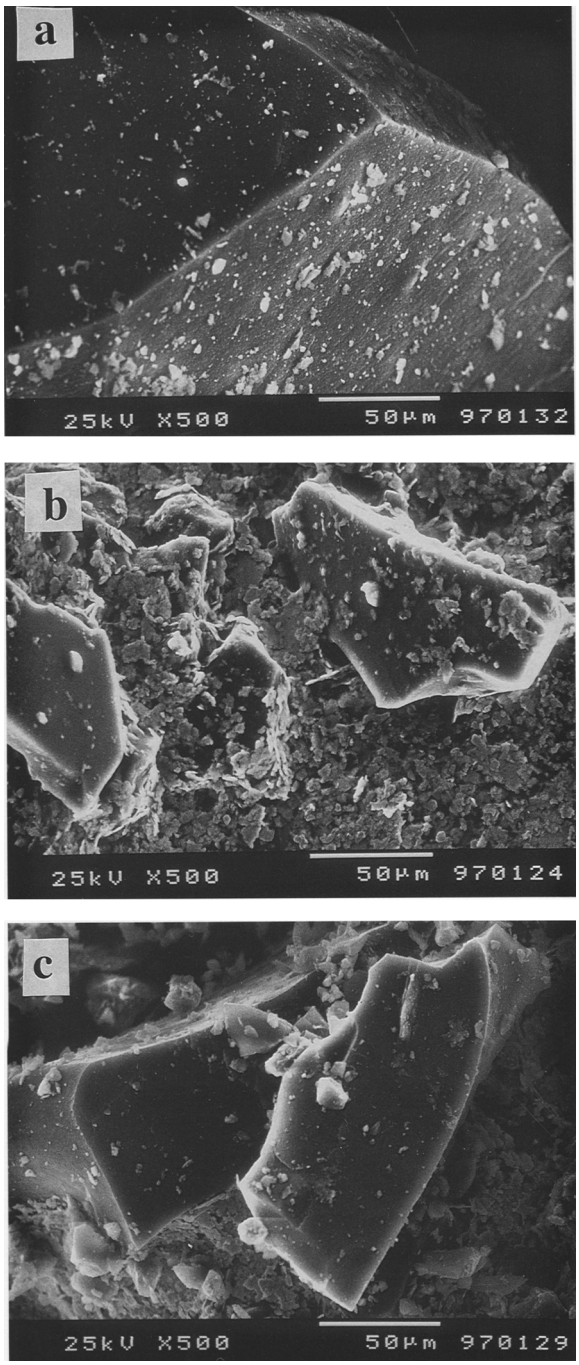

Figure 6. SEM images of a) HT sample, b) CHT calcined at 773 K and c) CHT calcined at 1073 K.

DISCUSSION

Information reported by Miyata (1983) for the Gaines-Thomas equilibrium constant (log Ke) for HT are: 1.84 for CO_3^{2-}, 1.42 for OH^- and −0.60 for I^-. These data show that selectivity follows the sequence $CO_3^{2+} > OH^- > I^-$. As HT exhibits a greater affinity towards divalent anions (Chatelet et al. 1996), and in particular towards CO_3^{2-}, it should be expected that exchange with I^- ions would be very weak. Accordingly, in our experiments the I^- sorption values were very low for HT (at 291 and 473 K). Oscarson et al. (1986) have found that HT did not remove detectable amounts of I^- from either deionized distilled water or a solution of NaCl (1 *M*). On the other hand, in CHT, when in contact with NaI solution, OH^- ions should be preferentially inserted in the structure. The I^- was preferentially adsorbed because its concentration is much higher than that of OH^-; that does not happen in NaI-1 solution, where I^- concentration was much lower than that of OH^-. The CHT can adsorb $^{131}I^-$ anions from the aqueous solution due to the reconstruction of the HT structure following the reaction proposed by Hermosin et al. (1993) for an organic anion:

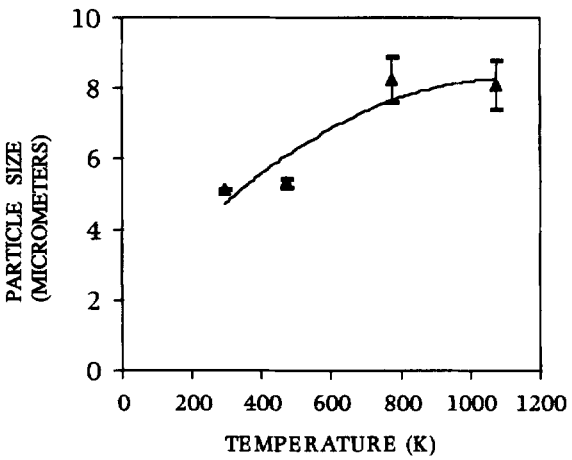

Figure 7. Particle size of CHT samples as a function of calcination temperature.

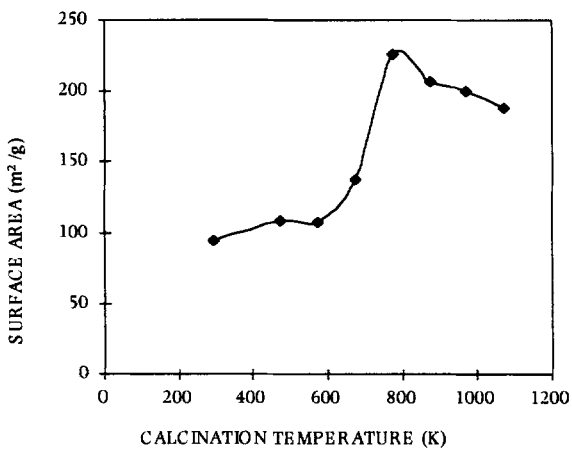

Figure 8. Surface area vs. the calcination temperature of the HTs.

https://doi.org/10.1346/CCMN.1998.0460510 Published online by Cambridge University Press

$$Mg_3AlO_4(OH) + 4H_2O + {}^{131}I^- \rightarrow (Mg_3Al(OH)_8)({}^{131}I) + OH^- \quad [1]$$

Although the amount of I^- sorbed by HT and CHT samples is very much dependent on the concentration of the NaI solutions, it is worthy of notice that the sorption behavior is similar in both cases, that is, in the very diluted carrier-free NaI-1 solution (10^{-14} *M*) and in the concentrated 0.1 *M* NaI solution. Figure 1 shows the similarity between both behaviors. The shape of both curves shows no dependency on the I^- concentration; I^- sorption is influenced strongly by the thermal treatment of the solids.

The pH increase of NaI-1 solution in contact with HT from 6.1 to 9.05, and of NaI-2 solution in contact with HT from 7.4 to 9.14, was probably due to a partial dissolution of the samples as stated by Hermosin et al. (1996). The increase of the pH value of the solutions in contact with the calcined samples can be attributed to the consumption of protons during the reconstruction of the layered structure (Sato and Okuwaki 1991; Hermosin et al. 1996). The different pH increments depend on the amount of HT reconstructed, which determines the I^- sorbed. Thus, the highest pH values were found for 773CHT and 873CHT samples.

Results of thermal analysis in the present work for HTs are in the range of those found by Miyata (1975, 1980). Reichle et al. (1986), Sato et al. (1986) and Rey et al. (1992) on HTs and Ulibarri et al. (1987) on pyroaurite. They differentiated 2 weight loss stages during the course of thermal decomposition of the layered double hydroxycarbonate: 1) interlayer water was lost around 470 K and 2) CO_2 was released from the interlayer region as well as H_2O from the brucite-like layer at around 650 K. In the present work, the first weight loss, at 473 K, has to be attributed to interlayer water desorption. Fifteen percent of the total weight in the original HT and 13% in the 773CHT-I samples were lost, which indicates the presence of less interlayer water in 773CHT-I. The second weight loss at 673 K corresponds to the dehydroxylation and decarbonation of the original HT and dehydroxylation, decarbonation and deiodination of 773CHT-I sample. Twenty-three percent in HT and 33% in 773CHT-I samples were lost, probably because I^- is much heavier (127 g eq^{-1}) than CO_3^{2-} ions (30 g eq^{-1}) or OH^- ions (17 g eq^{-1}).

The interplanar distances *d*(006) obtained by XRD given in Table 2 can be correlated to the ion sizes of the various anions. The $^{131}I^-$ monovalent ion (2.06 Å) is larger than the OH^- (1.18–1.23 Å) and the divalent ion CO_3^{2+} (1.85 Å). Therefore, a shift of the (006) diffraction peak towards higher angular values should be expected as the size of the anion incorporated into the HT network diminishes. From this criterion, I^- is incorporated into the interlayer space. The plot of *d*-values, Table 2, against calcination temperature reproduces, indeed, the shape of the curves of Figure 1.

From SAED patterns, in all cases, HT material was identified: hexagonal configuration in spot patterns and a high level of coincidences (higher than 90%) were found in most diffraction patterns (ICDD 22-700 and also 41-1428). It is important to remark that differences between the HT sample and the CHT sample after exchange with NaI solution showed no difference in the configuration. These results agree with that obtained by XRD showing the lamellar reconstruction of the HT.

Additionally, in some patterns, reflections coming from brucite and periclase were found in minor quantities. Analyses of diffraction patterns from laminate configurations like the ones presented in the 1073CHT sample showed the presence of γ-Al_2O_3, in small quantities. These results are similar to those obtained by XRD.

Choudhary and Pandit (1991) found that the surface area of MgO decreased considerably for increasing temperatures from, 873 to 1073 or 1173 K. The increase of BET surface area of HT sample on heating up to 773 K and then, on further heating to higher temperatures, the decrease of the surface area, have been described in the literature for various HT-like materials. In the present paper, we observed a similar tendency measured by BET surface area when the HT was calcined at different temperatures (Figure 8).

On studying pyroaurite (Ulibarri et al. 1987) it was found that, on increasing temperature, the BET surface area increased slowly and reached the maximum value at 873 K. Above that temperature, the specific surface area drastically diminished because of sintering of the sample and disappearance of its mesoporosity.

The shape of the curve showing surface BET evolution versus calcination temperature resembles that obtained for the I^- sorption curve (Figure 1). Hence, a clear correlation exists between the surface area of the solids and the I^- sorption. The increase of the surface area at 773 K reveals the formation of the MgO and Al_2O_3 oxide (as shown in Figure 3a) whose particle size is close to 7 μm (Figure 7). The $^{131}I^-$ in the aqueous phase can easily diffuse through them to reconstruct the lamellar structure of the HT samples. However, when calcination temperature increases from 873 to 1073 K, the surface area decreases as particle size grows and a mixture of MgO and Al_2O_3 is present (Rey et al. 1992). Due to both facts, the diffusion of $^{131}I^-$ (ion radius: 2.06 Å) is more difficult, but OH^- with a smaller ion radius (1.40 Å) is preferentially inserted for the reconstruction of the HT structure whose *d*(006) value (Table 2) is similar to the original sample. Miyata (1980) reported that the HT sample calcined at 1073 K reconstructed HT when it was hydrated at 353 K for 24 h; however, the new lattice parameters were larger than those of the original sample.

Sato et al. (1986 and references therein) found similar results to those found by us when they placed magnesium aluminum oxides prepared by calcination of HTs at various temperatures in 0.1 *M* disodium hydrogen phosphate solution to evaluate the capacity to take up phosphate. They found that the rate at which phosphate was taken up decreased with increasing calcination temperature. According to them, this result could be due to the grain growth of magnesium aluminum oxide caused by the higher calcination temperature. Their sample calcined at 1273 K, which was a mixture of MgO and Al_2O_3, did not take up phosphate ion. This result is similar to those obtained in the present paper for the I^- sorption by the HT.

CONCLUSIONS

The sorption of $^{131}I^-$ on HT samples depends strongly on the thermal treatment and also on their surface area. The highest $^{131}I^-$ sorption capacity is found for an HT structure destroyed at 773 K whose resulting surface area is the highest one. Therefore, I^- uptake on HTs can be improved by thermally treating the clays before the uptake process. In this way, the structure of the original HT is lost and magnesium and aluminum oxides derived from HTs are formed. As a consequence, the surface area of the mixture is increased, and the I^- ions have free access to the exchange centers. Furthermore, I^- ions react with the oxides and the structure is recovered by reconstruction of the layered structure, in the interlayer spacings, compensating the positive layer charge besides OH^- and residual CO_3^{2-} ions.

Similar iodide sorption behavior was found for very different NaI concentrations (10^{-14} and 10^{-1} *M*) for both HTs and their calcined products.

ACKNOWLEDGMENTS

We thank J. J. Fripiat for helpful suggestions and also the technicians of the Chemistry Department (ININ), V. H. Lara (UAM) and J. Cañetas (UNAM). Partial financial supports from the European Community (Contract Cl-l*-CT94-0064), the DGAPA (project IN106295) and the CONACYT (project 26769-E) are gratefully acknowledged.

REFERENCES

Atkins M, Glasser FP. 1990. Encapsulation of radioiodine in cementitious waste forms. In: Oversby VM, Brown PW, editors. Proc Mater Res Soc Symp; 1989; Pittsburgh, PA. p 15–22.

Cavani F, Trifiro F, Vaccani A. 1991. Hydrotalcite-type anionic clays: Preparation, properties and applications. Catal Today 11:173–301.

Chatelet L, Bottero JY, Yvon J, Bouchelaghen A. 1996. Competition between monovalent and divalent anions for calcined and uncalcined hydrotalcites: Anion exchange and adsorption sites. Colloids Surf A 111:167–175.

Choudhary UR, Pandit MY. 1991. Surface properties of magnesium oxide obtained from magnesium hydroxide Appl Catal 71:265–274.

Hermosin MC, Pavlovic I, Ulibarri MA, Cornejo J. 1993. Trichlorophenol adsorption on layered double hydroxide: A potential sorbent. J Environ Sci Health A 28:1875–1888.

Hermosin MC, Pavlovic I, Ulibarri MA, Cornejo J. 1996. Hydrotalcite as sorbent for trinitrophenol sorption capacity and mechanism. Water Res 30:171–177.

Kopka H, Beneke K, Lagaly G. 1988. Anionic surfactants between double metal hydroxide layers. J Colloid Interface Sci 123:427–436.

McKenzie AL, Fishel CT, Davis RJ. 1992. Investigation of the surface structure and basic properties of calcined hydrotalcites. J Catal 138:547–561.

Misra C, Perrotta J. 1992. Composition and properties of synthetic hydrotalcites Clays Clay Miner 40:145–150.

Miyata S. 1973. Synthesis of new hydrotalcite-like compounds and their physico-chemical properties Chem Lett X:843–848.

Miyata S. 1975. The synthesis of hydrotalcite-like compounds and their structures and physico-chemical properties-I: The systems Mg^{2+}-Al^{3+}-NO_3^-, Mg^{2+}-Al^{3+}-Cl^-, Mg^{2+}-Al^{3+}-ClO_4^-, Ni^{2+}-Al^{3+}-Cl- and $Zn^{2+}Al^{3+}$-Cl^-. Clays Clay Miner 23:369–375.

Miyata S. 1980. Physico-chemical properties of synthetic hydrotalcites in relation to composition. Clays Clay Miner 28: 50–56.

Miyata S. 1983. Anion exchange properties of hydrotalcite-like compounds. Clays Clay Miner 31:305–311.

Olguín MT. 1994. Fijación de uranio y productos de fisión del U^{235} en arcillas y zeolitas [Ph.D. thesis]. México, D.F.: Universidad Autónoma Metropolitana. 135 p.

Olguín MT, Solache-Ríos M, Iturbe JL, Bosch P, Bulbulian S. 1996. Sorption of ^{239}Np and ^{235}U fission products by zeolite Y, Mexican natural erionite and bentonite. Sep Sci Technol 31:2021–2044.

Oscarson DW, Miller HG, Watson RL. 1986. An evaluation of potential additives to a clay-based buffer material for the immobilization of I-129. Technical report. Atomic Energy of Canada Ltd, Whiteshell Nuclear Research Establishment. p 1–24.

Reichle WT. 1985. Catalysis reaction by thermally activated synthesis, anionic. Clay minerals. J Catal 94:547–557.

Reichle WT. 1986. Synthesis of anionic clay minerals (mixed metal hydroxides, hydrotalcite). Solid State Ionics 22:135–141.

Reichle WT, Kang SY, Fuerhardt DS. 1986. The nature of the thermal decomposition of a catalytically active anionic clay mineral. J Catal 101:352–359.

Rey F, Fornes V, Rojo JM. 1992. Thermal decomposition of hydrotalcites. J Chem Soc, Faraday Trans 88:2233–2238.

Sato T, Fujita H, Endo T, Shimada M, Tsunashima A. 1988. Synthesis of hydrotalcite-like compounds and their physico-chemical properties. React Solids 5:219–228.

Sato T, Kato K, Endo T, Shimada M. 1986. Preparation and chemical properties of magnesium aluminum oxide solid solutions. React Solids 2:253–260.

Sato T, Okuwaki A. 1991. Intercalation of benzenecarboxilate ions into the interlayer of hydrotalcite. Solid State Ionics 45:43–48.

Ulibarri MA, Hernández MJ, Cornejo J. 1987. Changes in textural properties derived from the thermal decomposition of synthetic pyroaurite. Thermochim Acta 113:79–86.

Received 6 June 1997; accepted 6 March 1998; Ms. 97-051